Investigation and design of high-speed transimpedance amplifier circuits using CFOAs

Ivailo M. Pandiev

The paper presents the structure and principle of operation of the basic transimpedance amplifier (TIA) circuits. In particular, high-speed (with bandwidth >1M*Hz) inverting and non-inverting circuits, employing current-feedback operational amplifier (CFOA) are under consideration. Based on analysis of the operational principle, equations for the frequency and step responses of both circuits are obtained. As well, approximate formulas for the related dynamic electrical parameters at simultaneously operation of the input, transmission and load parasitic capacities are worked out. The formulas for the step responses of the circuits are obtained from the transfer functions by applying the inverse Laplace transformation. Moreover, using these formulas a design procedure, valid for frequencies up to* 500M*Hz*, *is developed. The efficiency of the proposed procedure is demonstrated by simulation and experimental study of sample electronic circuits of TIAs. The comparative analysis shows that the maximum value of the achieved relative error between the calculated and the simulated results is less than 10%. Moreover, an error of 10% is quite acceptable, considering the technological tolerances of the parameters.*

Изследване и проектиране на високоскоростни трансимпедансни усилвателни схеми, използващи CFOAs (Ивайло М. Пандиев). *Статията представя структурата и принципа на работа на основните трансимпедансни усилвателни схеми (transimpedance amplifier – TIA circuits), По-конкретно, обект на разглеждане са високоскоростните (с честотна лента* >1M*Hz) инвертираща и неинвертираща схеми, използващи операционен усилвател с вътрешна токова обратна връзка. Въз основа анализ на принципа на работа на двете схеми са получени изрази за честотните и преходните характеристики, както и приблизителни формули за свързаните с тях електрически параметри при едновременното действие на входните, предавателните и изходните паразитни капацитети. Формулите за преходните характеристики на схемите са получени от предавателните функции чрез прилагане на обратната трансформация на Лаплас. При това, използвайки тези формули е развита методика за проектиране, валидна за честоти до около* 500M*Hz. Ефективността на предложената методика е демонстрирана чрез симулационно и експериментално изследване на трансимпедансни усилватели. Сравнителният анализ показа добро съвпадение, като постигнатата максимална относителна грешка между изчислените и симулационните резултати не надвишава* 10*%. Грешка със стойност, равна на* 10*%, е съвсем приемлива, имайки предвид технологичните допуски в параметрите.*

Introduction

The high-speed (with bandwidth >1M*Hz*) transimpedance amplifier (TIA) circuits are essential building blocks for D/A current-to-voltage converters, AM radio receivers and photodiode transimpedance amplifiers for optical transceivers. In the past two decades, several TIAs were proposed in the literature [1-5]. Also, recently in [6] and [7], as well as in some technical documents [8-9] design recommendations of TIAs were proposed. For all electronic circuits such as an active element a conventional voltage-feedback operational amplifier (VFOA) or a common source TIA with a shunt-feedback resistor (for frequencies higher than 1M*Hz*) is used. The main advantages of the TIAs with conventional operational amplifiers (op amps) are the small input and output impedance, also the circuits are with relatively simple structure and the methods for determining the values of the passive components are well developed in the literature. The

main drawback of VFOAs is the finite gain-bandwidth product. As a result, in the process of design and implementation the TIAs may need to be stabilized.

In [10], the authors proposed approaches aimed to design VFOA-based amplifiers with constant closed-loop bandwidth. One possible way to obtain such a behavior is performed by replacing the gain resistor of an inverting configuration with transconductor, based on OTA. Another approach suitable for discrete applications, presented in [10], uses two conventional op amps in a composite fashion to implement a current-feedback op amp – like amplifier.

In the past ten years monolithic current-feedback operational amplifiers (CFOAs) have been basically used as active building blocks for design of various high-speed analog circuits. As a kind of the monolithic operational amplifiers family, the CFOAs have been realized basically to overcome the finite gain-bandwidth product of the conventional VFOAs.

Relatively large number of books, publications and company application reports are devoted to the theory and the design of the amplifier circuits employing CFOAs. Despite increasing applications of the CFOAs in the theoretical analyzes first-order models of the amplifiers are most frequently used [11-18]. The simple CFOA models are suitable for analyzing the typical behaviour, but are not useful to study the stability of the circuits in a wide frequency range.

In 1996 Mahattanakul and Toumazou [12] presented, a comprehensive theoretical study of the stability of CFOAs, when used with both resistive and capacitive feedback. The paper are identified some of the most suitable features of designing circuits with CFOAs, and the impact of these features affecting the amplifiers stability. For the theoretical analysis a small-signal two pole model of CFOA is used. In this model the first pole is determined by r_t and C_t, while the second pole occurs due to the current-mirror circuit in the real part. Typically, the current-mirror pole frequency is much higher than the pole frequency due to the transimpedance pole of the amplifier. Unfortunately, the input parasitic capacities that can affect the stability of the amplifiers at higher frequencies are not taken into account.

In [13], an analysis of stability and compensation of CFOAs is presented. In the theoretical analysis of the inverting amplifier, integrator and differentiator using small-signal model of a CFOA, some of the input parasitic capacitances and the effect of the transmitssion and load capacitances are included. Moreover, the load is considered only as capacitance C_L without taking account the parallel connection of the resistance R_L and the capacitance C_L (i.e. $Z_L = R_L \| (1/sC_L)$). This study is particularly useful for pencil-and-paper design of CFOA and takes into account both the resistive and capacitive feedback.

In 2005, Pennisi proposed a CMOS CFOA that is robust and exhibits good performance in wide frequency range [15]. The solution is based on a class AB differential amplifier. The proposed amplifier is theoretically studied and the second-order transfer function is obtained. Based on the transfer function formulas for the dominant and second pole are obtained. The dominant pole is due to r_t and C_t, while the second pole is due to $r_{in}^- \| r_o$ and the load capacitance C_L.

In [11] and [14] CFOA-based current-to-voltage converters are presented. To ensure stable operation of the circuits compensation capacitors are connected in parallel with the feedback resistors. As a result, the bandwidth is limited, but a stable operation is provided. For the theoretical analysis and the formulas based on it, a simplified model of the amplifier is used, which does not consider several parasitic effects.

In [17], the author's attention is focused on the analysis and design of basic amplifier circuits using a simplified model of a CFOA. As a result are obtained first-order complex transfer functions, in which the parasitic effects influencing at higher frequencies (for frequencies higher than $50MHz$) are not taken into account. Furthermore are not addressed the problems associated with the stability analysis in wide frequency range of the circuits. In [19], depth study of stability analysis in a wide frequency domain is presented. In the analysis of the electronic circuits a complex CFOA model is used, in which the input, transmission and load parasitic capacities are taken into account. However, the proposed design methodology can not be used for the TIAs using CFOAs.

Recently, in [20] compensation techniques for improving amplitude and phase response of CFOA-based inverting amplifier are investigated. The compensation technique, proposed in the paper, employing composite CFOA consisting two monolithic op amps used in the place of single CFOA.

In the past few years, the TIAs are increasingly used in the data converters for amplifying pulse input currents $i_G(t)$ with small ($<10ns$) rise and fall times. In these cases, in the process of analysis and design it is essential to use the corresponding transient responses. Moreover, in a practical point of view is very important to determine the values of the electrical parameters at a unit input step excitation $i_G(t)$, where

$i_G = 1$ for $t \geq 0$ and $i_G = 0$ for $t < 0$. The transient responses of the TIAs can be obtained from the complex transfer functions by applying the inverse Laplace transformation. In [11], [16] and [18] the transient responses at various damping ratios ξ in a graphical form are presented and the influence of certain parameters of the amplifier circuits is briefly discussed. In [21], the authors have provided the transient response of second-order amplifier with two complex-conjugated poles. The influence of ξ on the output signal's form is discussed and formulas for the amplitude of the first peak at $\xi < 0{,}707$ are obtained. Furthermore, an approximate expression for the settling-time at $\xi < 1$ is proposed.

In this paper, using the features of the Cadence OrCAD® and relatively simple theoretical analyses, the author has attempted to clarify the processes developing in the basic TIAs, employing CFOAs, and also to propose a design procedure for calculation of the individual components. Moreover, it is shown that the TIAs can be implemented using CFOAs and thus the stability problems that are typically encountered at VFOA realization, are avoided.

Small-signal model of a CFOA

For the theoretical analyses in this work the small-signal model of a CFOA [19], [20], given in Fig. 1, is used. The CFOA is equivalent to a CCII+ plus an output voltage buffer. These op amps have a high impedance non-inverting input *y*, a low-impedance inverting input *x*, a current output *z* and the voltage output *o*. The port *z* is between the first stage (CCII+) and the second stage (voltage buffer), where the resistance is very high (magnitude of several mega ohms).

The model accurately describes the behaviour of a typical CFOA over a wide frequency range, including electrical parameters such as inverting and non-inverting input impedance, open-loop transimpedance and output resistance.

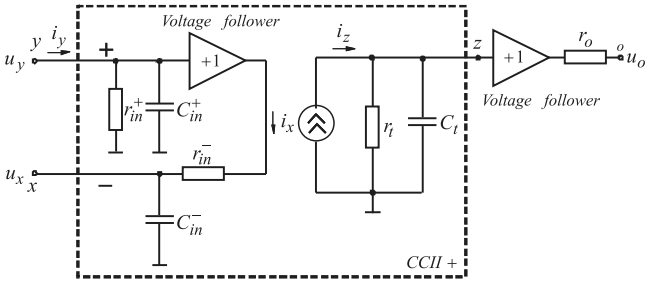

Fig. 1. A linear model of a monolithic CFOA.

The equivalent circuit of the model contains: input and output buffers with voltage gain equal to one; i_x and i_z – input and output current through the current-controlled current source – CCCS (or current mirror); r_{in}^{+} and C_{in}^{+} – resistance and capacitance of the non-inverting input; r_{in}^{-} and C_{in}^{-} – resistance and capacitance of the inverting input; r_t and C_t – equivalent to Z_t – transmission impedance; and r_o – output resistance.

The ideal relations between input and output voltages and currents can be given by the following hybrid matrix

$$(1) \qquad \begin{bmatrix} i_y \\ u_x \\ i_z \\ u_o \end{bmatrix} = \begin{bmatrix} 1/Z_{in}^{+} & 0 & 0 \\ 1 & Z_{in}^{-} & 0 \\ 0 & 1 & 1/Z_t \\ 0 & 0 & 1 \end{bmatrix} \begin{bmatrix} u_y \\ i_x \\ u_z \end{bmatrix},$$

where $Z_{in}^{+} = r_{in}^{+} \| (1/pC_{in}^{+})$, $Z_{in}^{-} = r_{in}^{-} \| (1/pC_{in}^{-})$ and $Z_t = r_t \| (1/pC_t)$.

To achieve simplicity of the mathematical equations (1) neglects several second-order effects found in the real CFOAs (such as the frequency dependence of the output impedance of the voltage followers, the *CMRR*, noise and the temperature effects).

Electrical circuits and theoretical analyses

Inverting circuit of transimpedance amplifier

The structure of the TIA employing CFOA is shown in Fig. 2. For low frequencies (approximately up to $10MHz$), the influence of the parasitic capacitances C_{in}^{+}, C_{in}^{-} and C_L can be neglected, thereby the real linear model of the CFOA (Fig. 1) is simplified. Then, for the transfer function (using the condition $r_o << r_t$) is given by the following approximate expression

$$(2) \qquad Z_{TR}(s) \approx Z_{TR}(0)/(s + \omega_p),$$

where $Z_{TR0} = R_F / \left[1 + \frac{R_F}{r_t} \left(1 + \frac{r_{in}^{-}}{R_F} \right) \left(1 + \frac{r_o}{R_L} \right) \right]$ is the DC transimpedance and $\omega_p = 1/R_F C_t \left(1 + \frac{r_o}{R_L} \right) \left(1 + \frac{r_{in}^{-}}{R_F} \right)$ is the pole frequency, defining working frequency bandwidth $\omega_{-3dB} = 2\pi f_{-3dB}$ of the circuit.

The value of the output offset voltage, determined by the input offset voltage U_{io} and the input bias current I_B^{-} to the inverting input of the CFOA for room

temperature (usually at $25°C$) is given by

$$U_{o,err} = [1 + (R_F / R_G)][U_{io} + (R_F \parallel R_G) I_B^-]. \quad (3)$$

At higher frequencies ($>10MHz$) on the transfer function affect the total input capacitance $C_T = C_G + C_M + C_{id}^-$, the transmission capacitance C_t and the load parasitic capacitance C_L. The total capacitance is form by: $C_{id}^- = C_{id} + C_{iCM}^-$ (C_{id} is the differential input capacitance and C_{iCM}^- is the common-mode input capacitance for the inverting terminal of the CFOA); C_G – equivalent capacitance of the input source and C_M – mounting parasitic capacitance (with values usually up to $3pF$ [8, 9]).

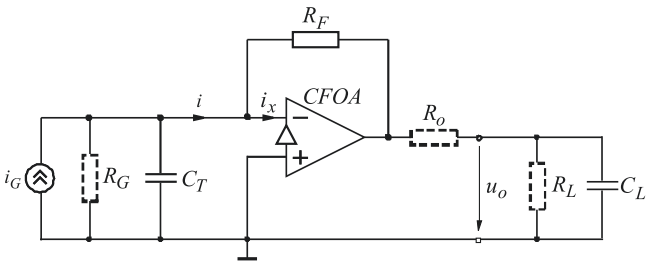

Fig. 2. An inverting circuit.

The analysis of the circuit in Fig. 2 is performed according to the method of the nodal voltages. The CFOA is replaced by the linear model, given in Fig. 1. The transfer function (using the condition $r_{in}^- << r_t$ and $r_{in}^- << R_G$) at $Z_L = R_L \parallel (1/sC_L)$ (the load impedance is a parallel connection of the load resistance R_L and the load capacitance C_L) is given by

$$Z_{TR}(s) \approx H\omega_p^2 (s - \omega_z) / \left(s^2 + \frac{\omega_p}{Q_p} s + \omega_p^2 \right), \quad (4)$$

where

$$H = C_t r_{in}^- r_o / \left[1 + \frac{R_F}{r_t} \left(1 + \frac{r_o}{R_L} \right) \right] \quad (5)$$

is the transmission coefficient,

$$\omega_z = R_F / (r_{in}^- r_o C_t) \quad (6)$$

is the zero angular frequency,

$$\omega_p = \sqrt{\frac{1 + \frac{R_F}{r_t}\left(1 + \frac{r_o}{R_L}\right)}{C_t r_{in}^- r_o \left[C_T \left(1 + \frac{R_F}{r_o}\right) + C_L \left(1 + \frac{R_F}{r_{in}^-}\right) + \frac{C_T C_L R_F}{C_t r_t} \right]}} \quad (7)$$

is the pole angular frequency (self-oscillating frequency or undamped natural frequency) and

$$Q_p = \frac{\sqrt{C_t r_{in}^- r_o \left[C_T \left(1 + \frac{R_F}{r_o}\right) + C_L \left(1 + \frac{R_F}{r_{in}^-}\right) + \frac{C_T C_L R_F}{C_t r_t} \right]}}{\left(R_F C_t + r_{in}^- C_t\right)\left(1 + \frac{r_o}{R_L}\right)} \quad (8)$$

is the quality factor of the transimpedance amplifier.

The analysis of formula (4) shows that the transfer function is characterized by one zero with positive real part (with angular frequency ω_z) and one double-pole (with angular frequency ω_p). The zero can be neglected since $\omega_p >> \omega_z$, as always satisfies the condition $\frac{\sqrt{r_{in}^- r_o}}{R_F} \sqrt{\frac{C_t}{C_T[1 + (R_F / r_o)] + C_L[1 + (R_F / r_{in}^-)]}} << 1$. Furthermore, the ω_z is a much larger than the $\omega_1 \approx 1/(r_{in}^- C_t)$, since r_{in}^- / R_F and $r_o << R_F$. In comparison, the noise gain (*NG*) of the VFOA-based TIAs has zero at $1/(R_F C_F)$ and pole at $1/[R_F(C_T + C_F)]$, as $\omega_z < \omega_p$. In order to maintain the stability, the noise gain slope has to be flattened by choosing an appropriate value of C_F for the optimum performance, such that noise gain is equal to the open-loop gain of the VFOA at $f_p = 1/2\pi(R_F C_F)$ [8] or by choosing the appropriate values for the DC gain and the dominant pole of the op amp [3]. As a result, at the point of intercept of the noise gain and the open-loop gain, the phase margin is approximately equal to $45°$.

Based on the complex function, the module and the phase shift of the CFOA-based TIA is given by

$$Z_{TR}(\omega) = \frac{H\omega_p^2}{\sqrt{\left(\omega_p^2 - \omega^2\right)^2 + \omega^2 \left(\omega_p / Q_p\right)^2}} \text{ and} \quad (9a)$$

$$\varphi_{Z_{TR}} = 180° - \arctan \frac{\omega_p \omega}{Q_p(\omega_p^2 - \omega^2)}. \quad (9b)$$

As a result of the theoretical analysis for the frequency bandwidth ω_{-3dB} is obtained [12]

$$\omega_{-3dB} = \omega_p \sqrt{\left(1 - \frac{1}{2Q_p^2}\right) + \sqrt{\left(1 - \frac{1}{2Q_p^2}\right)^2 + 1}}. \quad (10)$$

At $Q_p = 0{,}707$, formula (10) yields $\omega_{-3dB} = \omega_p$.

According to the type of the roots of the polynomial in the denominator of the transfer function (4), ap-

plying the Inverse Laplace Transform (ILT) of $R_U(s) = (1/s)Z_{TR}(s)$ is obtained two forms for the transient characteristic.

(1) *For complex-conjugated roots* ($0 < \xi < 1$ (or $Q_p > 0{,}5$), where $\xi = 1/(2Q_p)$ is the damping ratio) of the denominator a pseudo-periodic operation of the TIA is obtained and for the transient response can be written [21]

$$u_o = H\left[1 - \frac{1}{\sqrt{1-\xi^2}} e^{-\xi\omega_p t} \sin(\omega_p \sqrt{1-\xi^2}\, t + \theta)\right] i_G , \quad (11)$$

where $\theta = acr\tan(\sqrt{1-\xi^2}/\xi)$.

The rise time of the output signal is approximately defined as the time interval for which the sine component becomes zero (before the first peak) and has a value:

$$t_r \approx \pi\left(1 - \frac{acr\tan\sqrt{1-\xi^2}/\xi}{180°}\right)/[\omega_p\sqrt{1-\xi^2}]. \quad (12)$$

(2) *For simple real roots* ($\xi > 1$ or $Q_p < 0{,}5$) of the denominator, monotonically operation of the TIA is obtained and the transient response is given by

$$u_o = H\left[1 - \frac{\xi}{\sqrt{\xi^2-1}} e^{-\xi\omega_p t}\left(\frac{e^{\omega_p\sqrt{\xi^2-1}t}}{2(\xi-\sqrt{\xi^2-1})} - \frac{e^{-\omega_p\sqrt{\xi^2-1}t}}{2(\xi+\sqrt{\xi^2-1})}\right)\right] i_G . \quad (13)$$

Based on formula (13), *the rise time* is

$$t_r \approx 4{,}4/[\omega_p(\xi - \sqrt{\xi^2-1})]. \quad (14)$$

As can be seen in formula (14) the rise time increases, when ξ accept values higher than unity. In this case, the system is said to be *overdamped*.

Non-inverting circuit

Increased stability and the possibility of adjustment of the transmission ratio can be achieved with the non-inverting circuit, shown in Fig. 3. This circuit performs amplification after current-to-voltage conversion by a resistor R_G, there will be no damaging effects, which result from a phase shift of the op amp.

At higher frequencies (> 10M*Hz*) on the transfer function of the input network, and thus on the overall transfer characteristic of the systems of the amplifiers affect two capacitances: $C_P = C_{in}^+ + C_M$ and $C_N = C_{in}^- + C_M$. Also, the transfer function of the circuits is affected by the C_t and the load capacitance C_L. The analysis of the circuit is also performed according to the method of the nodal voltages and the op amp is replaced by the linear model, presented in Fig. 1. For the corresponding transfer function (using the condition $r_{in}^- << r_t$ and $r_o << r_t$) is found

$$Z_{TR}(s) \approx H\omega_{p,in}(s+\omega_z)/(s+\omega_{p,in})\left(s^2 + \frac{\omega_p}{Q_p}s + \omega_p^2\right). \quad (15)$$

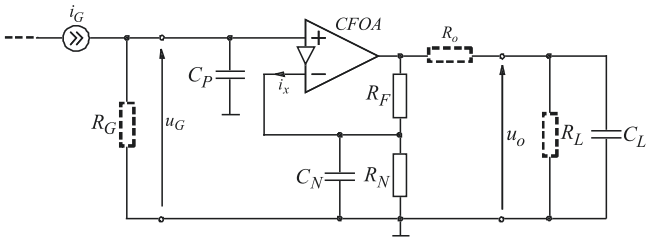

Fig. 3. A non-inverting circuit.

The formulas for the basic electrical parameters of this circuit are given in [19]. The DC transimpedance of the non-inverting circuit is

$$Z_{TR0} = (R_G \,||\, r_{in}^+)\frac{1 + R_F/R_N}{1 + \frac{R_F}{r_t}\left(1 + \frac{r_{in}^-}{R_N} + \frac{r_{in}^-}{R_F}\right)\left(1 + \frac{r_o}{R_L}\right)}. \quad (16)$$

To compensate the effect of the parasitic capacitance C_P, the resistor R_G have to be chosen with value $R_G << r_{in}^+$. Then, $\frac{1 + sR_GC_P}{1 + s[(r_{in}^+ \,||\, R_G)C_P]} \cong 1$ and $u_i \cong u_y$. In this compensation method the bandwidth is not narrowed and also the spikes are not reduced.

The step responses for the non-inverting circuit, using formula (15) and the ILT, can be written as:

(1) *For complex-conjugate roots* ($0 < \xi < 1$):

$$u_o \approx \frac{H\omega_z}{\omega_p^2}\left[1 - \frac{\omega_p}{\omega_z}\frac{1}{\sqrt{1-\xi^2}} e^{-\xi\omega_p t} \sin\left(\omega_p\sqrt{1-\xi^2}\, t + \frac{\pi}{2}\right)\right] i_G . \quad (17)$$

Based on the analysis of the above formula the following approximate formula can be written for the rise time:

$$t_r \approx \pi/(2\omega_p\sqrt{1-\xi^2}). \quad (18)$$

For $\xi \le 0{,}707$ (or $Q_p \ge 0{,}707$) and $\omega_p < \omega_z$ at a frequency equal to ω_p the denominator of a function (15) tends to zero and the voltage gain theoretically increases toward infinity. As a result, occurs peaking in the frequency and the step responses. Moreover, the circuit of the amplifier becomes unstable. Also, at

$\xi > 0{,}707$ and $\omega_z < \omega_p$ occurs ringing in the output signal, which can cause unstable operation of the circuit. In the both cases, the steady-state value of the output signal is reached after damped oscillations.

(2) *For simple real roots* ($\xi > 1$):

(19)
$$u_o \approx \frac{H\omega_z}{\omega_p^2}\left[1-\frac{\omega_p}{\omega_z}\left(\frac{e^{-(\xi\omega_p-\omega_p\sqrt{\xi^2-1})t}}{2\sqrt{\xi^2-1}}-\frac{e^{-(\xi\omega_p+\omega_p\sqrt{\xi^2-1})t}}{2\sqrt{\xi^2-1}}\right)\right] i_G .$$

The transient response consists of one DC component that determines the steady-state value, and has two exponents. The first exponent has smaller time constant and sets the initial increasing of the output signal. The second one has larger time constant and grows slower. Moreover, the second exponent was added to the first exponent and the sum of both components determined the output signal increasing. In this case, *the rise time* of the output signal can be obtained by the following approximate expression:

(20)
$$t_r \approx \sqrt{\left[\frac{2{,}2}{\omega_p\left(\xi-\sqrt{\xi^2-1}\right)}\right]^2+\left[\frac{2{,}2}{\omega_p\left(\xi+\sqrt{\xi^2-1}\right)}\right]^2} .$$

Design procedure

The purpose of computing is insight, not numbers.
Richard W. Hamming

The above analytical formulas, resulting of the theoretical analysis, are on the base of the proposed design procedure for TIAs, implemented with the circuits shown in Fig. 2 and Fig. 3. The created procedure consists of (1) preliminary hand calculations and (2) simulation testing of a prototype. The final results are analyzed an optimal variant for the circuit is chosen. The procedure for the preliminary hand calculations is based on the following sequence:

(1) *Technical specification*. The circuit elements are calculated using pre-defined: amplitude of the input current I_G with internal resistance R_G and internal parasitic capacitance C_G; input resistance r_{iA}; mounting parasitic capacitance C_M; amplitude of the output voltage U_{R_L} at load resistance R_L and load capacitance C_L; output resistance r_{oA}; frequency bandwidth f_{-3dB} (or $\omega_{-3dB} = 2\pi f_{-3dB}$); rise time t_r at unit input step; relative error ε_{io} [%] defined by the input offset voltage and current and signal-to-noise ratio SNR.

(2) *Selection of an electronic circuit*. An object of analysis and design is the TIAs, shown in Fig. 2 and Fig. 3. The inverting circuit (Fig. 2) provides less input impedance (the inverting input x is a virtual ground – $u_{yx} \approx 0$), while in the second circuit (Fig. 3) the input current i_G is previously converted into voltage $u_G = i_G R_G$. The resulting voltage is amplified by a non-inverting amplifier.

(3) *The op amp is selected*:

– Maximum output voltage $U_{om} \geq U_{R_L}$ (U_{om} is the maximum output voltage of the op amp);

– The power supply voltage $V_{CC} = -V_{EE}$ is selected higher than the maximum output voltage U_{om}, as saving the condition $V_{CC\min} < V_{CC} < V_{CC\max}$;

– Maximum output current $I_{o,\max} > I_L$, where $I_L = U_{R_L} / R_L$;

– Small-signal bandwidth $f_1 > (5...10) f_{-3dB}$, where f_1 is the unity-gain bandwidth;

– Slew rate $SR_{CFOA} > 2\pi f_{-3dB} U_{R_L}$.

(4) *The value of the equivalent quality factor and damping ratio of the frequency response are obtained*:

– For the inverting circuit (Fig. 2) by using formula
$$Q_p = \sqrt{\omega_{-3dB}}\,\frac{\sqrt{r_{in}^- C_T + r_o C_L + \dfrac{r_{in}^- C_T r_o C_L}{r_t C_t}}}{1 + r_o / R_L} \quad (\xi = 1/2Q_p);$$

– For the non-inverting amplifier (Fig. 3) by using formula
$$Q_p = \sqrt{\omega_{-3dB}}\,\frac{\sqrt{r_{in}^- C_N[1+(r_o/R_L)+r_o C_L/(r_{in}^- C_T)]}}{1+r_o/R_L} .$$

(5) *The feedback resistor R_F is calculated*:

– For the inverting circuit:
$$R_F \leq 1/\omega_p^2\left(r_{in}^- C_T C_t + r_o C_L C_t + r_{in}^- r_o C_T C_L / r_t\right);$$

– For the non-inverting circuit:
$$R_F \leq 1/\omega_p^2\{r_{in}^- C_t C_N[1+(r_o/R_L)+r_o C_L/(r_{in}^- C_T)]\} .$$

For the TIA, shown in Fig. 3, the R_G is calculated as follows: $R_G \leq 0{,}01 r_{in}^+$. The value of the gain resistor is $R_N = R_F/(A_{U0}-1)$, where $A_{U0} = U_{R_L}/U_G$.

The calculated values for the resistors R_F and R_N, according to the above formulas, have to be consistent with the values from the data-sheet of the chosen CFOA.

According to the obtained value of the quality factor, found in step № 4, the value of the self-oscillating frequency ω_p is given by:

– For the inverting circuit:

At $0<\xi<1$ $\omega_p = \pi \dfrac{1-\dfrac{acr\tan\sqrt{1-\xi^2}/\xi}{180^\circ}}{t_r\sqrt{1-\xi^2}}$;

At $\xi>1$ $\omega_p = 4{,}4[t_r(\xi-\sqrt{\xi^2-1})]$.

– For the non-inverting circuit:

At $0<\xi<1$ $\omega_p = \pi/(2t_r\sqrt{1-\xi^2})$;

At $\xi>1$

$$\omega_p = \sqrt{\left[\frac{2{,}2}{t_r\left(\xi-\sqrt{\xi^2-1}\right)}\right]^2+\left[\frac{2{,}2}{t_r\left(\xi+\sqrt{\xi^2-1}\right)}\right]^2}.$$

(6) *The input and output resistance is calculated*:

The input resistance of the circuits are: $r_{iA} \approx R_F / A_{d0}$ and $r_{iA} \approx R_G$, respectively.

The output resistances are:

$$r_{oA} \approx r_o\left(1+\frac{R_F}{R_G}\right)/A_{d0} \text{ and } r_{oA} \approx r_o\left(1+\frac{R_F}{R_N}\right)/A_{d0}.$$

(7) *The phase margin* (PM) *is calculated* at ω_{-3dB}:

– For the inverting circuit $\varphi_m = 180^\circ - \varphi_{Z_{TR}}(\omega_{-3dB})$;

– For the non-inverting circuit

$$\varphi_m = 180^\circ - \left[\arctan\left(\frac{\omega_{-3dB}}{\omega_z}\right) - \arctan\frac{\omega_p\omega_{-3dB}}{Q_p(\omega_p^2-\omega_{-3dB}^2)} - \arctan\left(\frac{\omega_{-3dB}}{\omega_{p,in}}\right)\right].$$

(8) *The output offset voltage of the circuit is calculated*: First the output offset voltage for room temperature (usually $25°C$) is calculated:

– For the inverting circuit by using formula (3);

– For the non-inverting circuit

$U_{o,err} = (1+R_F/R_N)[U_{io} + (R_F \| R_N)I_B^- - R_G I_B^+]$.

The relative error $\varepsilon_{io} = (U_{o,err}/U_{R_L})100\%$ is compared with the value, given in step № 1.

(9) *The signal-to-noise ratio* (*SNR*) is calculated:

– For the inverting circuit, first the resulting noise voltage at the TIA's output is calculated:

$U_{oN}^2 = U_{N,CFOA}^2 + I_{N,CFOA}^2 R_F^2 + 4kTR_F B_{eq}$,

where $U_{N,CFOA}$ and $I_{N,CFOA}$ are the noise voltage and the noise current of the op amp and $B_{eq} \approx 1{,}57 f_{-3dB}$ is the noise bandwidth.

Then, the signal-to-noise ratio (*SNR*) is given by

$SNR,\ dB = 20\lg(U_{o,eff}/U_{oN})$ [dB].

The value obtained of the calculation is compared with the specified in step № 1. If the result does not meet the specification, for example a more precise op amp can be selected.

– For the non-inverting circuit the resulting noise voltage at the output is calculated:

$U_{oN}^2 = U_{N,CFOA}^2 A_{U0}^2 + I_{N,CFOA}^2 R_F^2 + 4kTR_G B_{eq} A_{U0}^2 + 4kTR_F B_{eq} + 4kTR_N B_{eq}(R_F/R_N)^2$.

Simulation and experimental testing

To verify the theoretical analysis and the proposed procedure, in this section examples of studying of TIAs at several transimpedances are given. A wide bandwidth ($f_1 > 400MHz$) CFOA type AD8011 (from Analog Devices) is chosen as an active building block. The studies of sample TIAs (Fig. 2 and Fig. 3) are performed in two stages – simulation modeling and experimental testing.

The computer simulations of the circuits are performed by using AD8011AN PSpice macro-model (version 1.0). To obtain the frequency and step responses through simulation AC sweep and Transient analyses with combination of a parametric analysis are performed within OrCAD PSpice®.

For the experimental testing the TIAs were implemented on a FR4 PCBs laminate with SMD passive components. The AC transfer characteristics of the circuits experimentally, by using network analyzer HP4195A, are obtained.

In Table 1 for the inverting circuit, the calculated and simulation results at the R_F equal to $1k\Omega$, 750Ω and 500Ω are summarized. The simulations are performed at $I_G = 1mA$, $R_G = 0{,}1M\Omega$, $C_G = 1pF$, $C_M = 3pF$ and $Z_L = R_L \| C_L = 50\Omega \| 5pF$. At R_F equal to $1k\Omega$ and 750Ω, the peaks are not observed and the frequency response decreases monotonically with increasing the frequency of the input signal. Moreover, in these cases $Q_p < 0{,}7$ and $f_p < f_z$. As a result the circuits are stable ($\varphi_m > 45°$), without additional feedback capacitor C_F. At $R_F = 500\Omega$ the Q-factor becomes equal to 0.632, in the form of the frequency and step responses causes small peaking. At frequency equal to 226,4MHz $\varphi_m \approx 53°$. At further increase of the frequency the phase margin becomes smaller than 45°, which decreases the stability of the amplifier. Then, for $R_F \le 500\Omega$ $\varphi_m \le 45°$ and the TIAs becomes unstable.

The study of the non-inverting circuit (Fig. 3) is implemented at feedback resistor $R_F = 1k\Omega$ and 499Ω. In Table 2, at $R_F = 1k\Omega$, $R_G = 1k\Omega$,

$Z_L = 100k\Omega \,||\, 3pF$ – input impedance of the active probe type HP41800A and $C_M = 3pF$, the values of the dynamic parameters for gains A_{U0} equal to 1, 2, 6 and 11 of the amplifier stage are presented.

Table 1

Comparison between calculated and simulation results

Parameter	Calculated results	Simulation results
$R_F = 1k\Omega \pm 1\%$		
$Z_{TR0} / U_{o,err}$	998,9Ω / 7,125mV	998,8Ω / 7,113mV
f_z / f_p	842MHz / 183.3MHz	– / –
f_{-3dB} / φ_m	108,25MHz / 103,4°	104,7MHz / 100°
t_r	3,23ns ($\xi = 1{,}06$)	5,14ns
$R_F = 750\Omega \pm 1\%$		
$Z_{TR0} / U_{o,err}$	749,4Ω / 5,843mV	749,3Ω / 5,834mV
f_z / f_p	631MHz / 210,7MHz	– / –
f_{-3dB} / φ_m	148,7MHz / 85,3°	151MHz / 81,6°
t_r	6,02ns ($\xi = 0{,}937$)	6,45ns
$R_F = 500\Omega \pm 1\%$		
$Z_{TR0} / U_{o,err}$	499,7Ω / 4,562mV	499,7Ω / 4,554mV
f_z / f_p	421MHz / 255,6MHz	– / –
f_{-3dB} / φ_m	225,8MHz / 58,7°	226,4MHz / 53,3°
t_r	2,52ns ($\xi = 0{,}791$)	2,75ns

For $R_F = 1k\Omega$, at voltage gains A_{U0} of the amplifier stage equal to 1 and 2 in the form of the frequency and the time response causes peaking, and for the voltage follower the amplitude reaches approximately 15dB. Moreover, at gains 1 and 2, the module of the transfer function decreases with greater speed, such as for the frequency equal to 500MHz reaches value equal to –10dB. For A_{U0} equal to 1 and 2 $Q_p < 0{,}7$, but $f_z < f_p$. At gain equal to 1 the calculated and the simulation value is greater than 400MHz. The difference between the calculated and the experimental results is due to the influence of the additional parasitic poles, determined by the inertial intermediate stages of the real CFOA. At gains equal to 1 and 2, the phase shift between the input and the output signal is positive, because $f_z < f_p$. This additional phase shift has a value less than 50°, which does not affect on the stability of the circuits. For A_{U0} equal to 6 and 11 the bandwidth increased, but the frequency and the step responses are not ringing ($Q_p < 0{,}707$) and decreased monotonically with increasing the frequency of the input signal. Furthermore, the f_z is much greater than the f_p. The phase margin for the four gains is greater than 45°, which guarantee that the TIAs are stable, according to the Bode criterion. The comparative analysis shows that the relative error is less than 10%.

Table 2

Comparison between calculated and experimental results

Parameter	Calculated results	Simulation results	Experimental results
$A_{U0} = 1$, f_z =68,1MHz and f_p =285MHz.			
Z_{TR0}	998Ω	1,01kΩ	996Ω
Q_p	0,31	(the amount of peaking is 9,6dB)	(the amount of peaking is > 10dB)
f_{-3dB}	> 0,4GHz	> 0,4GHz	≈ 0,4GHz
t_r	3,57ns	2,61ns	-
$A_{U0} = 2$ ($R_N = 1k\Omega$), f_z =136MHz and f_p =282MHz.			
Z_{TR0}	1,996kΩ	2,01kΩ	1,992kΩ
Q_p	0.3	(the amount of peaking is small)	(the amount of peaking is small)
f_{-3dB}	239MHz	217MHz	220MHz
t_r	3,78ns	3,45ns	-
$A_{U0} = 6$ ($R_N = 200\Omega$), f_z =409MHz and f_p =273MHz.			
Z_{TR0}	5,98kΩ	6,01kΩ	5,94kΩ
Q_p	0,26	(without over-shoot)	(without over-shoot)
f_{-3dB}	78,9MHz	75MHz	72MHz
t_r	4,57ns	4,21ns	-
$A_{U0} = 11$ ($R_N = 100\Omega$), f_z =749MHz and f_p =262MHz.			
Z_{TR0}	10,97kΩ	10,97kΩ	10,93kΩ
Q_p	0,23	(the amount of peaking is small)	(the amount of peaking is small)
f_{-3dB}	63.2MHz	68MHz	60MHz
t_r	5,56ns	5,05ns	-

The smaller feedback resistance determined wider bandwidth and resulted in rise time decreasing. At $R_F = 499\Omega$ the rise time approximately varied from 1,8ns ($A_{U0} = 2$ – $R_N = 499\Omega$) to 3,2ns ($A_{U0} = 10$ – $R_F = 422\Omega \pm 1\%$, $R_N = 47{,}5\Omega$), while for $R_F = 1k\Omega$ the rise time is almost twice larger. Once again, the comparative analysis showed that the relative error for the rise time does not exceed 10%. This guarantees sufficient degree of accuracy.

Conclusion

In this paper the basic circuits of the TIAs, using CFOAs are discussed and analyzed. Based on the theoretical analyses formulas for the DC, AC and transient parameters are obtained. The proposed new expressions considered the physical parameters of the real CFOAs. Moreover, using the obtained formulas, a design procedure is developed and recommendations for stable operation are defined, in comparison to the

VFOA based realizations. The efficiency of the proposed procedure is demonstrated by analysis of concrete electronic circuits, using high-speed CFOA AD8011. The created approach can be useful for design of TIAs, employing in various mixed-signal systems.

REFERENCES

[1] Nguyen, D.B.Y, Q. Le, Y.-H. Oh, H.-B. Le. A high linearity, efficient bandwidth, and high stability transimpedance amplifier. In Proc. 48th Midwest Symposium on Circuits and Systems 2005, vol. 1, pp. 167-170.

[2] Ciofi, C., F. Crupi, C. Pace, G. Scandurra. A New Circuit Topology for the Realization of Very Low-Noise Wide-Bandwidth Transimpedance Amplifier. IEEE Transactions on Instrumentation and Measurement, vol. 56, no. 5, pp. 1626-1631, 2007.

[3] Säckinger, E., The Transimpedance Limit. IEEE Transactions on Circuits and Systems I: Regular Papers, vol. 57, no. 8, 2010, pp. 1848-1856.

[4] Y.-H. Kim, E.-S. Jung and S.-S. Lee. Bandwidth enhancement technique for CMOS RGC transimpedance amplifier. Electronics Letters, vol. 50, no. 12, 2014, pp. 882-884.

[5] Atef, M. High gain transimpedance amplifier with current mirror load. In Proc. 21st International Conference Mixed Design of Integrated Circuits & Systems (MIXDES), Lublin, Poland, 2014, pp. 220-223.

[6] Shahdoost, S., B. Bozorgzadeh, A. Medi, and N. Saniei. Low-noise transimpedance amplifier designing procedure for optical communications. In Proc. 22nd Austrian Workshop on Microelectronics (Austrochip), Graz, Austria, 2014, pp. 1-5.

[7] Shahdoost, S., B. Bozorgzadeh, A. Medi, and N. Saniei. A novel design methodology for low-noise and high-gain transimpedance amplifiers. In Proc. Argentine Conference on Micro-Nanoelectronics, Technology and Applications (EAMTA), 2014, pp. 77-82.

[8] Pachchigar, M.,Design considerations for a transimpedance amplifier. Application Report SNOA515A, Texas Instruments. [Online]. Available: http://www.ti.com/lit/an/snoa515a/ snoa515a.pdf.

[9] Designing photodiode amplifier circuits with OPA128. Application bulletin: SBOA061, Texas Instruments. [Online]. Available: http://www.ti.com/lit/an/sboa061/sboa061.pdf.

[10] Pennisi, S., G. Scotti, and A. Trifiletti. Avoiding the Gain-Bandwidth Trade Off in Feedback Amplifiers. IEEE Transactions on Circuits and Systems I: Regular Papers, vol. 58, no. 9, 2011, pp. 2108-2113.

[11] Franco, S. Analytical foundations of current-feedback amplifiers. In Proc. IEEE International Symposium on Circuits and Systems (ISCAS '93), Chicago, IL, vol. 2, 1993, pp. 1050-1053.

[12] Mahattanakul, J., and C. Toumazou. A theoretical study of the stability of high frequency current feedback op-amp integrators. IEEE Transactions on Circuits and Systems I: Fundamental Theory and Applications, vol. 43, no. 1, 1996, pp. 2-12.

[13] Palumbo, G. Current feedback amplifier: stability and compensation. In Proc. of the 40th Midwest Symposium on Circuits and Systems. Sacramento, CA, USA, vol. 1, 1997, pp. 249-252.

[14] Celma, S., F. Perez, and P.A. Martinez. Simple compensation techniques for current feedback op-amps. In Proc. IEEE International Conference on Electronics, Circuits and Systems, 1998, pp. 367-370.

[15] Pennisi, S. High-performance CMOS current feedback operational amplifier. In Proc. IEEE International Symposium on Circuits and Systems (ISCAS), vol. 2, 2005, pp. 1573 - 1576.

[16] Di Cataldo, G., A.D. Grasso, and S. Pennisi. Two CMOS Current Feedback Operational Amplifiers. IEEE Transactions on Circuits and Systems II: Express Briefs, vol. 54, no. 11, 2007, pp. 944-948.

[17] Pandiev, I., Analysis and design of CFOA-based high-speed amplifier circuits. In Proc. 20th Telecommunications Forum (TELFOR 2012), Belgrade, Serbia, 2012, pp. 979-982.

[18] Bayard, J. CFOA Based Inverting Amplifier Bandwidth Enhancement. IEEE Transactions on Circuits and Systems—II: Analog and digital signal processing, vol. 48, no. 12, 2001, pp. 1148-1150.

[19] Pandiev, I. Design and stability analysis of CFOA-based amplifier circuits using Bode criterion. Systems Science & Control Engineering: an open access journal, vol. 3, no. 1, 2015, pp. 367–380.

[20] Kamath, D. Bandwidth enhancement of inverting amplifier using composite CFOA block. International journal of innovative research in electrical, electronics, instrumentation and control engineering, vol. 2, no. 4, 2014, pp. 1387-1390.

[21] Laker, K.R., and M.C. Sansen. Feedback and sensitivity in analog integrated circuits and systems. in Design of analog integrated circuits and systems, Chapter 3. New York: McGraw-Hill, 1994, pp. 170-244.

Ivailo M. Pandiev *was born in Sofia, Bulgaria, in 1971. He received his BSc and MSc degrees in electronic and automation engineering from the Technical University of Sofia, Bulgaria in 1996 and Ph.D. degree in electronic engineering from the same university, in 2000. Since 2005, he is an associate professor in Analog and Mixed-signal (analog and digital) Electronics with the Department of Electronic Engineering. His research interests include: analysis, design and behavioral modeling of analog and mixed-signal circuits and systems.*

tel.: (02) 965 3027. *e-mail: ipandiev@tu-sofia.bg.*

Received on: 04.01.2016